



Article

Medical Cyclotron Solid Target Preparation by Ultrathick Film Magnetron Sputtering Deposition

Hanna Skliarova ^{1,*}, Sara Cisternino ^{1,*}, Gianfranco Cicoria ², Mario Marengo ²,
Emiliano Cazzola ³, Giancarlo Gorgoni ³ and Vincenzo Palmieri ^{1,†}

¹ Legnaro National Laboratories, Italian National Institute for Nuclear Physics (LNL-INFN), Viale dell'Università, 2, 35020 Legnaro (PD), Italy

² Medical Physics Department University Hospital "S. Orsola–Malpighi", 40138 Bologna, Italy; cicoria.gianfranco@aou.mo.it (G.C.); mario.marengo@unibo.it (M.M.)

³ IRCCS Sacro Cuore Don Calabria Hospital, Cyclotron and Radiopharmacy Department, 37024 Negrar (VR), Italy; Emiliano.Cazzola@sacrocuore.it (E.C.); giancarlo.gorgoni@sacrocuore.it (G.G.)

* Correspondence: Hanna.Skliarova@lnl.infn.it (H.S.); Sara.Cisternino@lnl.infn.it (S.C.); Tel.: +39-049-806-8416 (H.S. & S.C.)

† Deceased 16 March 2018.

Received: 22 December 2018; Accepted: 8 March 2019; Published: 13 March 2019



Abstract: Magnetron sputtering is proposed here as an innovative method for the deposition of a material layer onto an appropriate backing plate for cyclotron solid targets aimed at medical radioisotopes production. In this study, a method to deposit thick, high-density, high-thickness-uniformity, and stress-free films of high adherence to the backing was developed by optimizing the fundamental deposition parameters: sputtering gas pressure, substrate temperature, and using a multilayer deposition mode, as well. This method was proposed to realize Mo-100 and Y-nat solid targets for biomedical cyclotron production of Tc-99m and Zr-89 radionuclides, respectively. The combination of all three optimized sputtering parameters (i.e., 1.63×10^{-2} mbar Ar pressure, 500 °C substrate temperature, and the multilayer mode) allowed us to achieve deposition thickness as high as 100 μm for Mo targets. The 50/70- μm -thick Y targets were instead realized by optimizing the sputtering pressure only (1.36×10^{-2} mbar Ar pressure), without making use of additional substrate heating. These optimized deposition parameters allowed for the production of targets by using different backing materials (e.g., Mo onto copper, sapphire, and synthetic diamond; and Y onto a niobium backing). All target types tested were able to sustain a power density as high as 1 kW/cm² provided by the proton beam of medical cyclotrons (15.6 MeV for Mo targets and 12.7 MeV for Y targets at up to a 70- μA proton beam current). Both short- and long-time irradiation tests, closer to the real production, have been realized.

Keywords: cyclotron solid target; radioisotope production; magnetron sputtering; thick film deposition

1. Introduction

A conventional medical cyclotron solid target comprises the target material deposited onto a baking plate that is cooled by water from the back and possibly by helium gas flow from the front. There is a number of techniques for accelerator target preparation based on chemical, mechanical, or physical processes [1]. The list of the most common methods for cyclotron solid target production includes, but is not limited to, rolling or mechanical reshaping, pressing, sintering, electrodeposition, and a set of “physical” methods [2]. Here, we have associated with the group of physical methods different Physical Vapor Deposition (PVD) methods, such as Focused Ion Beam (FIB) or magnetron sputtering, thermal spray deposition, and plasma spray deposition. Table 1 presents a summary of the most commonly used methods for cyclotron solid target preparation and some examples of their

application for the preparation of Y and Mo targets, which is the topic of this work. A more detailed overview of Mo cyclotron solid target preparation has been presented recently by the authors [3]. Each method can be used either separately or in a combination with others, for example, pressing or electrophoresis followed by sintering [4], sintering followed by press-bonding [5,6], etc., which can lead to improved thermomechanical performance. The choice of a suitable method for target production is guided by the type of precursor material, target dimensions, desired backing plate, and the dissolution and separation procedures of the irradiated target. The optimal thickness of the target for radionuclides production depends on the preferred particle energy range, chosen in a way to minimize impurities. Usually, it is on the order of hundreds of micrometers or even millimeters. Material losses during the target preparation procedure should be minimized when costly isotopically enriched materials are used for production. Besides that, the target must be mechanically stable and able to withstand the thermodynamic conditions that occur during irradiation: no peeling, sputtering, evaporation, and other thermal damages should occur. Of course, performance under the beam depends on the irradiation parameters (beam energy and beam current).

An “ideal” technique, available for all types of materials and fulfilling all the requirements for the target, does not exist. The choice of technique for target preparation is always a compromise between the approach to fulfilling the particular requirements of each application and the cost of implementation.

Table 1. Comparison of the most common target preparation methods.

Method	Thickness	Deposited Material's Limitations	Backing	Losses	Example Mo, Y
Rolling (mechanical reshaping)	tens of μm ... mm	Metals, sufficiently ductile, not oxidized	Press-bonding to a backing is possible for soft materials.	10%–20%	[7–9]
Pressing	hundreds of μm ... mm	Not possible for hard materials without a binder	No backing. Press-bonding or brazing can be used as a second step of target preparation	<5%	[2,5,10]
Sintering	hundreds of μm ... mm	Oxygen-sensitive materials can be sintered either in a reduced atmosphere or by particular methods	No backing. Press-bonding or brazing can be used as a second step of target preparation	<5%	[11–13]
Melting	hundreds of μm ... mm	For high-melting-temperature materials, laser melting should be used	Melting temperature of backing is preferred to be higher than precursor material	<5%	[14,15]
Sedimentation	tens of μm ... hundreds of μm	A binder is needed	Various backing	<5%	[4,16]
Electrodeposition	μm ... hundreds of μm	Metals or oxides. Metals with high affinity to O cannot be deposited in pure form	Must be electrically conductive	10%–20%	[17,18]
“Physical” deposition *	μm ... hundreds of μm	Various materials	Various backing	70%–80%	[3,19–24]

* Here, physical deposition methods include different Physical Vapor Deposition (PVD) methods: Focused Ion Beam (FIB) and magnetron sputtering, thermal spray deposition, and plasma spray deposition.

In order to maximize the nuclear reaction yield, production should be performed at maximum proton currents. This means that the target system should provide high efficiency of heat dissipation. In order to achieve this purpose, the materials should have maximum thermal conductivity, including both the target material itself and the target backing plate, and should be connected by a method providing good thermomechanical contact between them. Direct deposition by sputtering may be particularly interesting in cases where: a relatively thin layer of target material is required and obtaining the proper contact between the target material and the backing is critical; the backing is cumbersome (particular, not disklike, shapes, such as microchannel- or metallic-foam-based heat exchanger as a part of the backing, etc.); or the alternative target bonding involves the use of material or processes that may introduce impurities (e.g., brazing, etc.).

The LNL-INFN group, in the framework of the LARAMED (LABoratories for RADioisotopes of MEDical interest) project [25], has proposed to use magnetron sputtering to deposit the target material

onto the appropriate backing plate in order to provide high density, high thickness uniformity, and high adherence to the backing. An innovative study of the Mo cyclotron solid target concept for ^{99m}Tc production was recently presented in [3]. This included sputter deposition of Mo target material onto a composite high thermal conductivity and chemical resistance backing plate. The previous article [3] was devoted to Mo deposition and the technological aspects of vacuum brazing to realize a composite backing plate. The scope of the present work is instead focused on the deposition method development.

In this work, the method originally developed to produce a Mo cyclotron solid target has been tested for another precursor material, Y for ^{89}Zr radionuclide production. Some technical details on Mo target preparation are repeated in the current work to compare the main deposition parameters for Y and Mo in order to illustrate the versatility of the developed method, its applicability to different target and backing materials, and its capability to produce targets for different target stations.

Both radionuclides ^{99m}Tc and ^{89}Zr have importance for medical applications. The interest in additional/alternative routes for ^{99m}Tc production has been stimulated by the perceived new ^{99m}Tc crisis, due to the scheduled shutdown of the Chalk River nuclear power plant in 2018. Cyclotron-based production of ^{99m}Tc , starting from ^{100}Mo by $^{100}\text{Mo}(p,2n)^{99m}\text{Tc}$ reaction, has been developed and evaluated at the LNL-INFN in the framework of the APOTEMA-TECHN_OSP project [25–30]. Regarding ^{89}Zr , the main interest in this radionuclide is related to the radiolabeling of slowly accumulating radiopharmaceuticals (*in vivo* imaging of antibodies, nanoparticles, and other large bioactive molecules) for targeting tumor cells [31–34]. The latter goal requires the ready availability of relatively large amounts of ^{89}Zr with high specific activity: this remains nowadays a challenge.

Magnetron sputtering is a very flexible PVD technique that allows to modify a lot the properties of the deposited film by changing the sputtering parameters. Magnetron sputtering is generally known as a PVD technique for the deposition of thin metallic films. However, it is not used for thick film deposition because of the tensile or compressive stress that is always present in the films [35,36]. Controlling the stress in PVD films is extremely important because of its close relationship to the technological properties of the material; the adhesion strength to the substrate; and the limit of film thickness without cracking, buckling, or delamination.

One of the most challenging issues of this study was to develop a method to deposit dense stress-free films of refractory metal with a thickness of the order of tens or even hundreds of microns. Magnetron sputtering was used to deposit a thick target film directly onto a backing plate. This approach could have a further advantage: to simplify the often-underestimated challenge of establishing good thermal contact between the target and the target backing plate.

Thus, in this work, the validation of the solid target production technology based on the magnetron sputtering technique was realized for both Mo and Y target preparation. Indeed, a set of Mo and Y target prototypes has been realized and successfully tested under the cyclotron's beam. The results have shown that the developed solid target preparation method is attractive for further optimization and implementation in medical radionuclide production.

2. Materials and Methods

2.1. Materials

Natural molybdenum (99.99% purity, Mateck GmbH, Julich, Germany), natural yttrium (99.9% purity, Gambetti Kenologia Srl, Binasco, MI, Italy), and argon (99.99% purity, SIAD S.p.A., 159 Bergamo, Italy) were used for sputtering deposition as target materials and sputtering gas, respectively.

Different substrate materials were used: Mo was deposited onto copper ($\text{Ø}32 \times 1$ mm), sapphire ($\text{Ø}12.7 \times 0.5$ mm, Meller Optics Inc., Providence RI, USA), chemical vapor deposited (CVD) synthetic diamond ($\text{Ø}13.5 \times 0.3$ mm, II-VI Advanced Materials GmbH, Pine Brook, NJ, USA), and silicon wafers of 50.8 mm diameter and 250–300 μm thickness of semiconductor quality and (100) orientation (Sil'tronix Silicon Technologies, Archamps, France).

Niobium disks of 99.9% purity ($\text{Ø}24 \times 0.5$ mm, Goodfellow Cambridge Ltd., Huntingdon, England) were used as the substrates for the yttrium deposition.

Copper substrates were washed in an ultrasonic bath for 20 min with GP 17.40 SUP soap (NGL Cleaning Technology SA, Nyon, Switzerland) and deionized water. This was followed by chemical etching with SUBU5 solution (5 g/L of sulfamic acid, 1 g/L of ammonium citrate, 50 mL/L of butanol, 50 mL/L of H_2O_2 , and 1 L of deionized water) at 72 ± 4 °C in order to remove surface oxides, passivation in 20 g/L of sulfamic acid, ultrasonic washing with water for 20 min, rinsing with ethanol, and drying with nitrogen.

Niobium and nonmetallic substrates cleaning procedure included: ultrasonic bath cleaning with Rodaclean® (NGL Cleaning Technology SA, Nyon, Switzerland) soap for 20 min at 40 °C; ultrasonic bath cleaning with deionized water for 20 min at 40 °C; rinsing with ethanol (storage in ethanol in plastic box); mechanical cleaning with ethanol and AlfaWipe® (Texwipe Company, Hoofddorp, The Netherlands); and drying with nitrogen gas immediately before positioning onto the substrate-holder.

2.2. Deposition System

The sputtering process was carried out in a cylindrical, stainless-steel vacuum chamber that was 25 cm in diameter and 25 cm in length. A base pressure of 5×10^{-6} mbar was reached without backing out (heating the vacuum flanges up to 200 °C to improve degassing during pumping) by means of the Pfeiffer turbo molecular pump of 360 L/min and the Varian Tri Scroll Pump of 210 L/min as a primary.

The films were deposited by DC (direct current) sputtering with a 2-in. planar magnetron cathode source unbalanced of the II Type. The depositions were performed onto planar substrate-holders, with a distance of 6 or 7 cm from the cathode.

The “down-top” deposition configuration, with the magnetron source placed from the downside of the cylindrical chamber and the substrate-holder with substrates from the top of the chamber, was used for the film deposition in order to minimize the film delamination probability caused by the metallic dust particles (Figure 1).

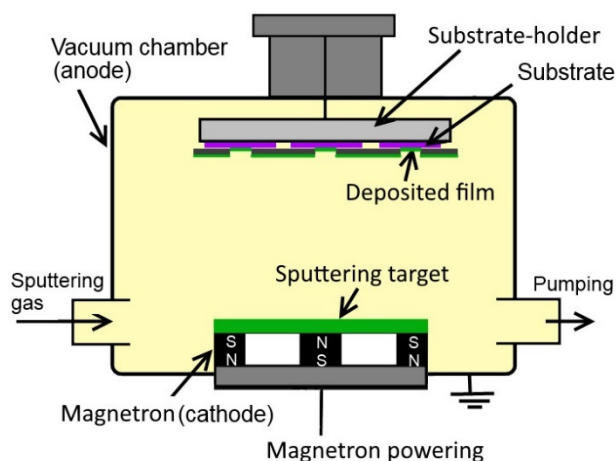


Figure 1. Scheme of “down-top” configuration.

The deposition onto 7/8 substrates was realized at the same time. The sputtering materials were deposited on a spot that was 10 mm in diameter in the center of each substrate (backing plate) defined by appropriate masks (Figure 2). For the Mo deposition, a 450-W Infrared (IR) lamp (Helios Italquarz, Cambiago-MI, Italy) was used to heat up the substrate-holder, and a K-type thermocouple, placed inside the furnace, was used to control the temperature with an automatic custom-made infrared lamp backing control system.

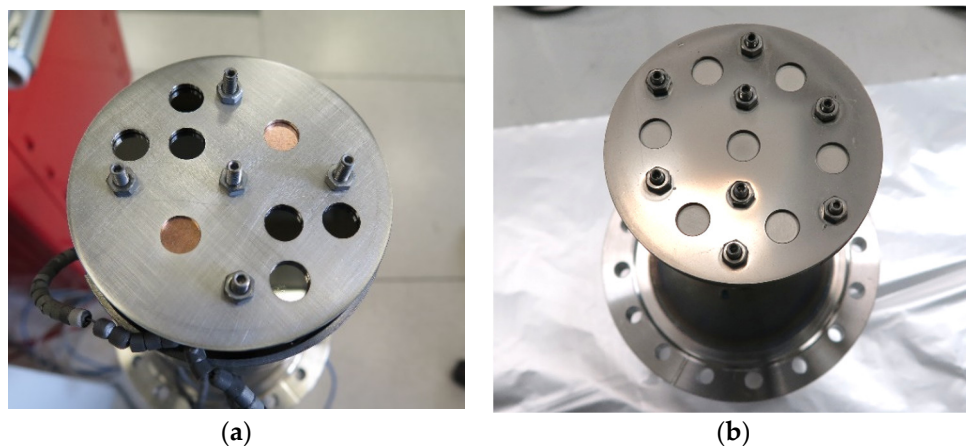


Figure 2. Masks assembled on heated substrate-holder for Mo sputtering (a) and on nonheated substrate-holder for Y sputtering (b).

2.3. Deposit Analysis

The evaluation of the film thickness was performed by the contact stylus profiler model Dektak 8 (Veeco, Plainview, NY, USA).

FEI (formerly Philips, OR, USA) Scanning Electron Microscope SEM XL-30 was used for the sputtered film analysis. Samples of 5- μm Mo film onto a silicon wafer substrate and 40- μm Y film onto a copper substrate were prepared in separate runs with the same optimized parameters for SEM cross-section analysis.

2.4. Cyclotron Tests

In this study, two different cyclotrons with the corresponding solid target stations were used for testing the Mo and Y sputtered targets. The Mo target irradiation tests were performed at the Medical Physics Department of “S. Orsola-Malpighi” Hospital in Bologna using the PETtrace 800S cyclotron (GE Healthcare, Chicago, IL, USA) equipped with the solid target station prototype of TEMA Sinergie S.P.A. (Faenza, Ra, Italy). The Y targets were tested under the TR19 cyclotron with the corresponding target station (ACSI, Richmond, BC, Canada).

The GE PETtrace 800S cyclotron (GE Healthcare, Chicago, IL, USA) works at a fixed proton energy of 16.5 MeV (deuteron energy 8 MeV) and currents up to 100 μA (the maximum current available practically depends on the source and tuning of the magnets). The solid target station (prototype TEMA Sinergie S.P.A., Faenza, Ra, Italy) is shown in Figure 3a. The target “coin” is cooled directly by the He gas flow in the front and indirectly through contact with the water-cooled aluminum chamber from the back. A detailed description of this irradiation unit was reported previously by Cicoria and co-workers [37,38].

TR19 14–19 MeV is a variable energy proton cyclotron with a high current ion source up to 300 μA . The corresponding ACSI solid target station allows for direct helium gas cooling of the target coin from the front part and water cooling from the back.

The target coin prototypes were realized fitting the design of the corresponding target station, which means disks of 2 mm maximum thickness and diameters of 32 mm (TEMA) and 24 mm (ACSI).

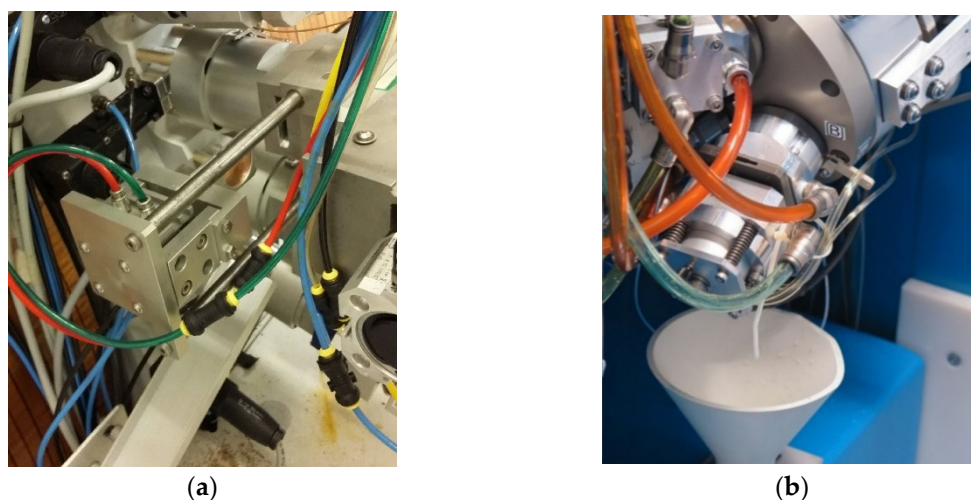


Figure 3. Solid target stations used for under-beam target tests: (a) TEMA Synergie target station prototype of PETtrace cyclotron (S. Orsola-Malpighi Hospital, Bologna); (b) TR19 cyclotron target station (Sacro Cuore Hospital, Negrar, Verona).

The irradiations of the target prototypes for thermomechanical stability control were carried out at 15.6 MeV for the Mo targets and 12.7 MeV for the Y targets at increasing currents. Irradiating for 60 s is sufficient to reach thermal equilibrium in the target. Even such short-time tests are sufficient to reveal the structural characteristics of the target depending on the backing material, the quality of deposition, adherence, etc. Indeed, the target “failing” (i.e., when the deposited layer is detached or cracked) occurs within the first 20 s of irradiation. In practice, an irradiation time of 0.5–2.0 h, or even more, is routinely adopted to allow the production of clinically relevant amounts of radionuclides. Then, the long-term stability of the target withstanding the short-time test is mainly determined by the stability of the beam and the cooling system. For this reason, the irradiation time of 1–2 min was chosen for the initial thermomechanical tests.

After each irradiation, the sample was unloaded to visually inspect the integrity of the target and the adhesion of the Mo or Y film on the backing. Longer irradiations were performed using one of the CVD synthetic-diamond-based Mo target prototypes (30 min at 15.6 MeV, 60 μ A, the maximum current reached by the cyclotron at that moment) and two Y targets (5 h, 12.7 MeV, 50 μ A).

2.5. Estimation of ^{89}Zr Expected Yields

In this study, the ^{89}Zr activity at the end of bombardment (EOB) of Y sputtered targets was not measured experimentally. Instead, it was predicted by means of the Radionuclide Yield Calculator (RYC) 2.0 software [39] containing SRIM (The Stopping and Range of Ions in Matter [40]) modules. The experimental nuclear cross-section data, presented in Experimental Nuclear Reaction Data (EXFOR [41]) and previously reported by Omara et al. [42], Satheesh et al. [43], and Zhao et al. [44] fit by Gaussian generalized distribution (GGD), were utilized for the calculations. In order to validate the calculations obtained using the RYC 2.0 software, the A_{theor} (this work) was compared to the data presented in the literature A_{theor} (Lit.).

In order to compare the produced Y targets with the ones reported in the literature, the EOB thick target yield for 1 h of irradiation was also estimated according to Equation (1), as suggested by Otuka et al. [45]:

$$a(t_{1h}) = \frac{A(t_{\text{irrad}})(1 - e^{-\lambda t_{1h}})}{I_0(1 - e^{-\lambda t_{\text{irrad}}})}, \quad (1)$$

$$\lambda = \frac{\ln 2}{T_{1/2}} \quad (2)$$

where $A(t_{irrad})$ is the experimentally measured ^{89}Zr activity at the end of bombardment (mCi) after t_{irrad} (h) irradiation at I_0 irradiation current (μA), $t_{1h} = 1$ h of normalizing irradiation time (h), λ is the radioactive decay constant, and $T_{1/2}$ is the ^{89}Zr radioactive half-life ($T_{1/2} = 78.4$ h).

While the tests reported in the literature $a(t_{1h})$ were calculated using reported experimental ^{89}Zr EOB activity A_{exp} , for Y-2 and Y-7 targets, instead, A_{theor} (this work) was used to predict the $a(t_{1h})$, since no experimental measurement of produced activity was realized.

3. Results and Discussion

3.1. Sputtering Parameters Optimization

Besides the classical stress-associated problems (e.g., cracking in the deposit or substrate, cracking at the substrate–deposit interface, and adhesion problems [46]), the stress in deposited films can be a reason for poor adhesion between a film (target material) and a substrate (backing plate). The thermal resistance of this contact can drastically increase, causing a decrease in heat exchange efficiency. Thus, the optimization of the Mo and Y deposition parameters, aiming to reduce stress, was mandatory for the purpose of this work (i.e., cyclotron solid target realization). The sputtering deposition process of Mo and Y, using the same 2-in. magnetron and the same vacuum chamber, is shown in Figure 4.



Figure 4. Plasma of Mo (a) and Y (b) during the sputtering process.

The intrinsic stress in PVD-deposited films depends on the energy supplied to the growing film surface during the deposition process. The parameters considerably involved in the change of the supplied energy and, thus, in the microstructure growth mechanism are the sputtering gas pressure, the temperature of the holder, bias, etc.

Theoretically, if the other sputtering parameters are kept fixed, there is a particular gas pressure that corresponds to the transition between the tensile and compressive stresses. High pressure corresponds to the decrease of the kinetic energy of sputtered atoms and reflected neutrals bombarding the growing film due to the increased frequency of the collisions with the sputtering gas. In this case, a more porous microstructure is created, which is attributed to tensile intrinsic stress. At low pressure, the arriving particles have higher kinetic energy, and a more dense film, usually with compressive stress, is created [47]. In the current work, the optimal pressure was achieved experimentally by performing short depositions (15 min) of the material of interest (Mo, Y) onto a flexible substrate (Kapton), keeping all the other deposition parameters fixed. The radius of curvature assumed by the Kapton is an indicator of the stress (see Figure 5).

In this way, the “transition” pressure for Mo deposition was found to be 1.63×10^{-2} mbar (corresponding to 17 sccm Ar gas flow) and 1.36×10^{-2} mbar (corresponding to 19 sccm Ar gas flow) for Y deposition. It should be noted that the distance from the magnetron to the substrate was slightly different in the two cases—6 cm for Mo deposition and 7 cm for Y deposition—due to the difference in the design of the substrate-holders.

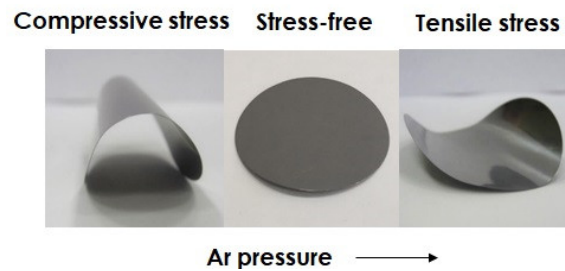


Figure 5. Kapton substrate curvature vs. sputtering pressure.

The second parameter, which strongly influences the intrinsic stress in films, is the substrate temperature, since it influences the kinetic energy of the particles that have already arrived at the substrate: the higher the temperature, the higher the density, thanks to renucleation. The transition homologous temperature $T_h = T/T_m = 0.2-0.45$ (where T is the temperature during vacuum deposition and T_m is the melting point of a deposited material), presented in the Structure Zone Model as the T-zone [35], corresponds to a transition from a tensile stress, attributed to the porous microstructure, to a near-zero or even low-level compressive stress of the dense bulk-like film. In this work, deposition was realized at the homologous temperature $T_h = T/T_m = 0.2$; this means $\sim 500\text{ }^\circ\text{C}$ for Mo and $\sim 250\text{ }^\circ\text{C}$ for Y. Indeed, the columnar dense microstructures of Mo and Y films (see Figure 6) obtained at $T_h = 0.2$ corresponded to the standard T-zone in the Structure Zone Model [35].

Table 2. Sputtering process parameters.

Parameters	natMo	natY
Argon flux (sccm)	17	19
Ar pressure (mbar)	1.63×10^{-2}	1.36×10^{-2}
Power (W)	5–550	400
Target-substrate distance (cm)	6	7
Substrate temp-re ($^\circ\text{C}$)	500	No heating
Deposition rate ($\mu\text{m}/\text{min}$)	11	13.3
Multilayer mode	Yes	No

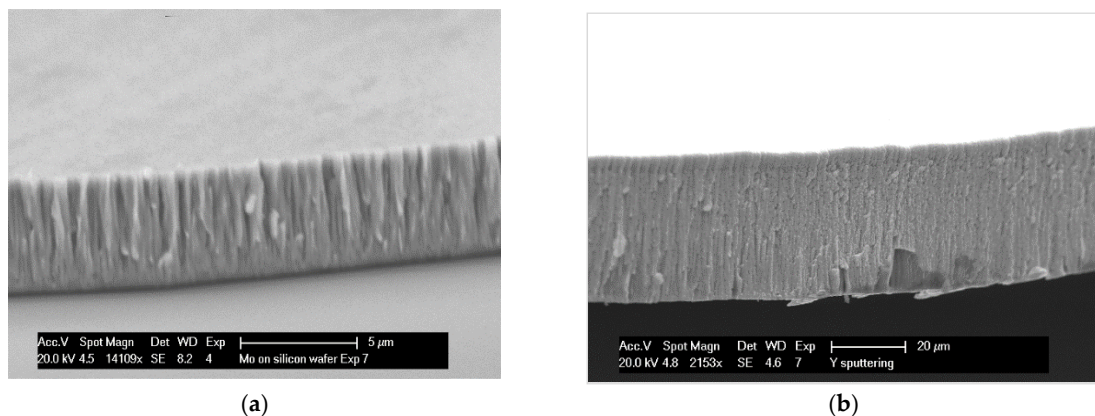


Figure 6. Cross-section SEM analysis of Mo film deposited onto Si at $500\text{ }^\circ\text{C}$ (a) and Y film deposited onto copper without forced heating ($220-250\text{ }^\circ\text{C}$) (b).

Furthermore, a multilayer deposition technique was shown to reduce the stress [48]; thus, the deposition of Mo thick films was fragmented in thousands of subsequent brief depositions of thin films, using an automatic program to control the power. Each deposition was interspersed by a “relaxation time” (80% duty cycle for a 1-min period), in which the film was annealed.

The optimized parameters for magnetron sputtering of both Mo (using copper backing, complex sapphire, or synthetic-diamond-based backing) and Y (on niobium backing) for the described deposition system configuration are shown in Table 2.

The deposition of Mo at 1.63×10^{-2} mbar Ar sputtering gas pressure, keeping the substrate-holder heated at 500 °C in a multilayer deposition mode (more details are presented in a previous work by the authors [3]), gave the best over 100- μm -thick Mo films in terms of adhesion, density (more than 95% of the bulk material), and being stress-free. It should be said that, in the past, a much lower Mo thickness of about 0.1 mg/cm² ($\sim 0.1 \mu\text{m}$ calculated for bulk density Mo), obtained using FIB [24] and ultrahigh vacuum sputtering [23], was reported. Our film thickness is comparable to the 130- μm Mo deposited by thermal spray deposition reported by Jalilian et al. [22]. All eight samples deposited in each sputtering run with the sample-holder (Figure 2a) have been characterized by high film-thickness uniformity.

The fact that ultrathick Mo films were deposited onto ceramic substrates, such as sapphire and CVD synthetic diamond, without stress-induced damage of the substrate demonstrates the versatility of the developed sputtering method. Indeed, the use of chemically inert backing materials (i.e., ceramics) in the dissolution process after target irradiation [30] would avoid radiochemical impurities in the final injectable radiopharmaceutical [3,49].

Instead, the thick stress-free Y films were obtained by merely optimizing the sputtering pressure. Since yttrium is very sensitive to oxidation, the multilayer mode was not applied in order to avoid the introduction of oxide layers between the metallic ones, which might promote the increase of intrinsic stress (and further possible delamination) instead of stress relaxation. Furthermore, the use of the floating temperature of the substrate-holder during the sputtering process simplified the system configuration from the point of view of hardware and safety. On the other hand, forced heating of the substrate-holder was not required in the case of Y sputtering, since the T_m of Y is lower than the one of Mo, and $T_h = 0.2$ was reached thanks to the interaction of the substrate-holder with plasma during the sputtering process.

Seven Y targets were produced in one deposition run. The sputtering deposition of six targets resulted in $\sim 50\text{-}\mu\text{m}$ -thick Y films, with a uniform distribution of film thickness. Only the target placed in the central position during the sputtering process showed a higher but less uniform thickness (70 μm). A representative example of the Y film profile sputtered onto 0.5-mm-thick niobium backing is shown in Figure 7. For Y targets, the niobium backing was chosen since it is inert in concentrated HCl, which was the media used for dissolution after irradiation [34].

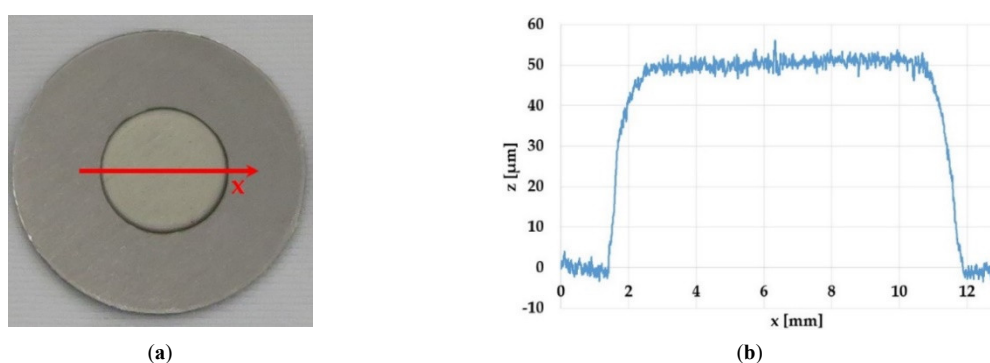


Figure 7. Deposited target profile measurement. (a). Yttrium sputtered target and profile measurement coordinate X (b). Typical target profile: X-measurement position, Z-height.

It should be noted that the main defect of the magnetron sputtering deposition technique is the great loss of the deposited material. Therefore, for a very expensive material, such as ^{100}Mo (starting material for cyclotron-produced $^{99\text{m}}\text{Tc}$ through $^{100}\text{Mo}(p,2n)$ nuclear reaction), the development of a suitable strategy for the deposition of a small amount of material and an efficient recovery method is

necessary. Instead, magnetron sputtering can be a powerful technique for materials with 100% natural abundance, such as ^{89}Y for the production of ^{89}Zr when a high yield of production is requested.

3.2. Cyclotron Test

The thermomechanical stability of the Mo targets produced by magnetron sputtering was evaluated under the beam of a 16-MeV GE PETtrace cyclotron, in the S. Orsola-Malpighi Hospital, Bologna, at 15.6 MeV, increasing the beam currents with 10- μA steps for 1 min irradiation, starting from 20 up to 70 μA (see Table 3). Visual control of the target after each irradiation was carried out.

All Mo target prototypes, based on about 100- μm -thick Mo film deposited by magnetron sputtering onto copper backing directly and ceramic (sapphire and CVD synthetic diamond) substrates brazed to the copper supports [49], showed good thermomechanical stability under the proton beam. The prototypes could sustain a power density of about 1 kW/cm^2 , provided by a proton beam of 15.6 MeV, 60 μA , and a spot size of ~ 11 mm diameter. Excellent adhesion (no delamination) and no film damage were observed after each irradiation. Only one of the sapphire-based samples was cracked, and in our interpretation, this was due to a problem during the brazing process, and not due to the irradiation. In fact, further CVD diamond-based targets were improved by adjusting the parameters of Ti metallization prior to brazing. A more detailed description of the results on different Mo target prototypes is presented in the previous work by the authors [3].

Y targets were irradiated under a ~ 10 mm in diameter proton beam of the TR19 cyclotron at 12.7 MeV at increasing currents up to 70 μA . The irradiation data are presented in Table 3. It is worth noting that the Y foil targets (thickness from 0.15 to 1 mm) commonly used by different groups to produce ^{89}Zr [19,38,50–53] can sustain, without any critical damage, only currents under 40 μA . Instead, the targets realized in this work have supported up to 1 kW/cm^2 heat power density, corresponding to relatively higher current values, which can increase the ^{89}Zr radioisotope production yields. Besides that, the thermomechanical performance of the targets realized using the method described in this work is comparable to one of the commercial sputtered Y targets [19]. Indeed, the integrity of the irradiated targets was not compromised, despite a visible dark spot in the center of the target corresponding to the beam profile, as shown in Figure 8. The white spot in the center of some targets can be explained by the creation of some amount of Y oxide/hydroxide due to water leakages in the target station.

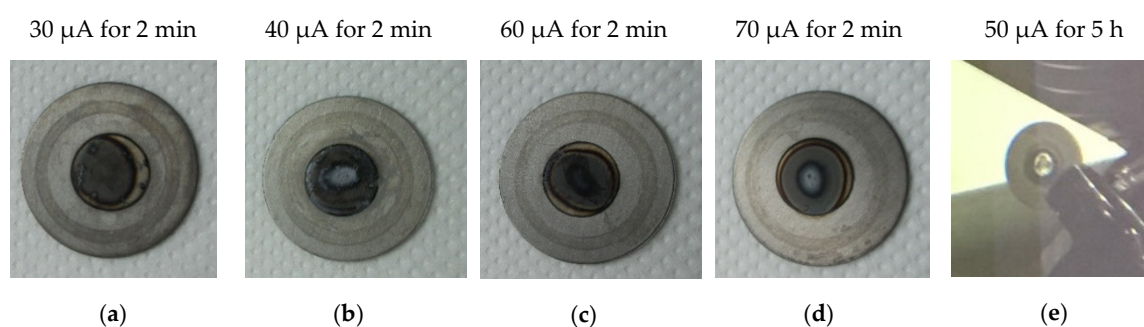


Figure 8. Y sputtered solid targets after irradiation under the 12.7-MeV proton beam of the TR19 ASCI cyclotron (Negrar, Verona, Italy): (a) Y-1, (b) Y-3, (c) Y-4, (d) Y-5, and (e) Y-7.

Table 3. Irradiation tests.

Target	Deposit Thickness	Backing	Beam Energy	Proton Current	Irradiation Time	Heat Power Density	Result
Mo-1	110 μm	Cu $\text{Ø}32 \times 1.5 \text{ mm}$	15.6 MeV	70 μA	1 min	1.2 kW/cm ²	Withstood
Mo-2	110 μm	Sapphire $\text{Ø}12.7 \times 0.5 \text{ mm}$ brazed to Cu $\text{Ø}32 \times 1.5 \text{ mm}$	15.6 MeV	60 μA	1 min	1 kW/cm ²	Withstood
Mo-3	125 μm	Diamond $\text{Ø}13.5 \times 0.3 \text{ mm}$ brazed to Cu $\text{Ø}32 \times 1.5 \text{ mm}$	15.6 MeV	60 μA	1 min	1 kW/cm ²	Withstood
Mo-4	125 μm		15.6 MeV	60 μA	30 min	1 kW/cm ²	Withstood
Y-1	50 μm	Nb $\text{Ø}24 \times 0.5 \text{ mm}$	12.7 MeV	30 μA	2 min	0.5 kW/cm ²	Withstood (Figure 8a)
Y-2	50 μm		12.7 MeV	50 μA	5 h	0.8 kW/cm ²	Withstood
Y-3	50 μm		12.7 MeV	40 μA	2 min	0.65 kW/cm ²	Withstood (Figure 8b)
Y-4	50 μm		12.7 MeV	60 μA	2 min	1 kW/cm ²	Withstood (Figure 8c)
Y-5	50 μm		12.7 MeV	70 μA	2 min	1.1 kW/cm ²	Withstood (Figure 8d)
Y-6	50 μm		12.7 MeV	70 μA	2 min	1.1 kW/cm ²	Withstood (Figure 8d)
Y-7	70 μm		12.7 MeV	50 μA	5 h	0.8 kW/cm ²	Withstood (Figure 8e)

The expected ⁸⁹Zr activity at the EOB estimated using the RYC 2.0 software is reported in Table 4. Since for the experiments reported by Queern et al. [19] some discrepancies were found only for higher-thickness targets of >200 μm (probably due to the chosen nuclear cross-section target datasets), the RYC 2.0 was found effective to predict the ⁸⁹Zr EOB activity of the Y-2 and Y-7 target irradiation experiments. Thus, the ⁸⁹Zr activities of about 41 and 57.2 mCi are expected to be produced irradiating Y-2 of 50 μm and Y-7 of 70 μm sputtered targets for 5 h at 12.7 MeV and 50 μA .

Table 4. Comparison of ⁸⁹Zr activity produced using sputtered targets.

Y Thickness, μm	Cyclotron, Target	E, MeV	I, μA	t, h	A_{exp}^1 , mCi	A_{theor}^2 (Lit.) mCi	A_{theor}^3 (this work) mCi	$a(t_{1h})^4$ mCi/ μA	Lit. Ref.
50	ACSI TR-19	12.7	50	5	-	-	41.0	0.16	This work
70		12.7	50	5	-	-	57.2	0.22	
110	ACSI TR-24, non-inclined target	12.5	10	0.5	1.63	1.82	1.8	0.33	[19]
140		12.5	21	0.5	3.94	4.86	4.8	0.37	
90		12.5	30	0.5	2.6	4.46	4.42	0.17	
220		12.5	40	2	25.37	31.28	55.2	0.31	
210		12.8	45	2	43.8	45.27	60.5	0.49	
90		12.8	40	2	21.9	23.09	23.8	0.28	
25 (700 eff. ⁵)	Philips AVF cyclotron, 1°–2° inclined target	14	100	1	130	-	184.3	1.3	[20]
35 (1000 eff. ⁵)		14	65–80	2–3	180–360	-	243.1–446.9	1.39–1.51	[21]

¹ A_{exp} —⁸⁹Zr measured activity at the end of bombardment (EOB), reported in the literature. ² A_{theor} (Lit.)—calculated ⁸⁹Zr activity at the EOB, reported in corresponding literature reference. ³ A_{theor} (this work)—⁸⁹Zr activity at the EOB, calculated with the RYC 2.0 software. ⁴ $a(t_{1h})$ —1-h EOB thick target yield. ⁵ eff.—effective thickness for inclined target calculated as deposit thickness divided into $\sin(2^\circ)$.

The ⁸⁹Zr 1-h EOB thick target yields $a(t_{1h})$ for Y-2 and Y-7 targets (see Table 4) were a bit lower but of the same order of magnitude with the thick target yields obtained by 90–220 μm ACSI commercial targets [19] and an order of magnitude lower than the ones produced irradiating 25/35- μm Y targets, as reported by Meijs et al. [20] and Verel et al. [21]. This can be explained by higher irradiation energy and the use of a low-angle inclined target configuration, since the effective target thickness is much higher in those cases.

Further depositions are planned to increase the thickness of the Y sputtered film in order to compete better with the commercially available targets. Besides that, new irradiations are required to assess the produced activity and the radionuclide purity in order to confirm the sputtering technique as an alternative route for the realization of Y targets for ⁸⁹Zr production [19–21].

4. Conclusions

The developed magnetron sputtering technique was successfully applied to the preparation of Mo and Y solid medical cyclotron targets, since this deposition method offers high density of the target material and high adherence to different backing materials. In this way, the good heat transfer allows for increasing the beam current during the irradiation. Indeed, realized solid targets can sustain up to a 1-kW/cm² proton beam heat power density with no critical damage. In addition, the capability to realize sputtered film onto any substrate gives the possibility of choosing the most suitable backing material for the purpose which each radionuclide production requires (i.e., thermal conductivity, chemical inertness). Thus, sapphire and synthetic diamond materials, inert in H₂O₂, which was the dissolution media for irradiated Mo targets, were used as the backing for the Mo targets, and Nb, inert in concentrated HCl used in the case of Y targets, was chosen as the backing for the realization of the Y targets. The performance of the homemade Y sputtered cyclotron solid targets was comparable to the commercial ones.

⁸⁹Zr activity of the order of 40–50 mCi is predicted to be produced by irradiating realized targets for 5 h at 12.7 MeV and 50 μA. The estimated 1-h EOB thick target yield is lower than the one of the ACSI commercial sputtered targets, but can be improved by increasing the Y layer thickness.

The versatility of the developed magnetron sputtering method has been proven in this study, and it can also be a promising alternative for other solid target materials.

5. Patents

The method for solid cyclotron target preparation reported in this manuscript was submitted by Istituto Nazionale di Fisica Nucleare on 14.09.17 as an Italian patent application, N. 102017000102990, dep. ref. P1183IT00, inventors V. Palmieri, H. Skliarova, S. Cisternino, M. Marengo, G. Cicoria, entitled “Metodo per l’ottenimento di un target solido per la produzione di radiofarmaci”. It was extended to the international patent application PCT/IB2018/056826, dep. ref. P1183PC00, on 07.09.18, entitled “Method for obtaining a solid target for radiopharmaceuticals production”.

Author Contributions: Conceptualization of the innovative cyclotron solid target prototype described in current work was done by H.S. and V.P.; the methodology for ultrathick Mo film deposition by magnetron sputtering was developed single-handedly by H.S.; further validation of the developed target preparation technique was realized by H.S. and S.C.; investigation of the performance of new target prototypes under cyclotron irradiation was performed by a group of collaborators, including H.S., S.C., M.M., G.C., E.C., and G.G.; resources of material science research lab and cyclotron facilities were provided by V.P., M.M., and G.G., correspondingly; data curation was under the responsibility of H.S., S.C., and E.C.; original draft preparation was performed by H.S. and S.C.; writing—review & editing by H.S., S.C., M.M., and E.C.; work on visualization was realized by H.S. and S.C.; V.P. formally, being responsible for the laboratory, and H.S. informally were in charge of work supervision and administration; funding acquisition was made by V.P.

Funding: The part of the research on Mo target preparation was realized in the framework of the TECHN_OSP project funded by CSN5 of the Istituto Nazionale di Fisica Nucleare, Italy for 2015–2017. National responsible: J. Esposito, LNL-INFN. The part on Y target preparation was a part of the Terabio INFN project, funded by the Italian Ministry. National responsible: V. Palmieri.

Acknowledgments: Special thanks should be given to Juan Esposito, responsible for the CSN5 INFN project TECHN_OSP, for his precious support, fruitful discussion during paper revision, as well as the funding acquisition. We are grateful to the staff of the LNL-INFN laboratories for the Surface & Material Treatments and for Nuclear Physics and Mechanical workshop for their help. We acknowledge the support and contribution of Stephen Jewkes in reviewing the language of this manuscript. We wish to thank also Anna Taffarello for her contribution to the English language and style editing.

Conflicts of Interest: The authors declare no conflict of interest.

References

1. Stolarz, A. Target preparation for research with charged projectiles. *J. Radioanal. Nucl. Chem.* **2014**, *299*, 913–931. [[CrossRef](#)] [[PubMed](#)]
2. IAEA. *Cyclotron Based Production of Technetium-99m*; IAEA: Vienna, Austria, 2017; ISBN 978-92-0-102916-4.

3. Skliarova, H.; Cisternino, S.; Cicoria, G.; Marengo, M.; Palmieri, V. Innovative Target for Production of Technetium-99m by Biomedical Cyclotron. *Molecules* **2019**, *24*, 25. [[CrossRef](#)] [[PubMed](#)]
4. Schaffer, P.; Benard, F.; Buckley, K.R.; Hanemaayer, V.; Manuela, C.H.; Klug, J.A.; Kovacs, M.S.; Morley, T.J.; Ruth, T.J.; Valliant, J.; et al. Processes, systems, and apparatus for cyclotron production of technetium-99m. Patent US 2013/0301769 A1; United States: TRIUMF, 14 November 2013.
5. Gagnon, K.; Wilson, J.S.; Holt, C.M.B.; Abrams, D.N.; McEwan, A.J.B.; Mitlin, D.; McQuarrie, S.A. Cyclotron production of ^{99m}Tc: Recycling of enriched ¹⁰⁰Mo metal targets. *Appl. Radiat. Isot.* **2012**, *70*, 1685–1690. [[CrossRef](#)] [[PubMed](#)]
6. Wilson, J.; Gagnon, K.; McQuarrie, S. Production of technetium from a molybdenum metal target. Patent US 2014/0029710A1; United States: University of Alberta, 30 January 2014.
7. Stolarz, A.; Kowalska, J.A.; Jasiński, P.; Janiak, T.; Samorajczyk, J. Molybdenum targets produced by mechanical reshaping. *J. Radioanal. Nucl. Chem.* **2015**, *305*, 947–952. [[CrossRef](#)] [[PubMed](#)]
8. Morrall, P.S. The Target Preparation Laboratory at Daresbury. *Nucl. Instrum. Methods Phys. Res. Sect. Accel. Spectrometers Detect. Assoc. Equip.* **2008**, *590*, 118–121. [[CrossRef](#)]
9. Manenti, S.; Holzwarth, U.; Loriggiola, M.; Gini, L.; Esposito, J.; Groppi, F.; Simonelli, F. The excitation functions of ¹⁰⁰Mo(p,x)⁹⁹Mo and ¹⁰⁰Mo(p,2n)^{99m}Tc. *Appl. Radiat. Isot.* **2014**, *94*, 344–348. [[CrossRef](#)] [[PubMed](#)]
10. Zweit, J.; Downey, S.; Sharma, H.L. Production of no-carrier-added zirconium-89 for positron emission tomography. *Int. J. Rad. Appl. Instrum. [A]* **1991**, *42*, 199–201. [[CrossRef](#)]
11. NISHIKATA, K.; Kimura, A.; Ishida, T.; KITAGISHI, S.; Tsuchiya, K.; Akiyama, H.; Nagakura, M.; Suzuki, K. Method of producing radioactive molybdenum. Patent US 13675769; United States. Japan Atomic Energy Agency, 30 May 2013.
12. Zeisler, S.K.; Hanemaayer, V.; Buckley, K.R. Target system for irradiation of molybdenum with particle beams. Patent US 2017/0048962A1; United States: TRIUMF, 16 February 2017.
13. Schaffer, P.; Bénard, F.; Bernstein, A.; Buckley, K.; Celler, A.; Cockburn, N.; Corsaut, J.; Dodd, M.; Economou, C.; Eriksson, T.; et al. Direct Production of ^{99m}Tc via ¹⁰⁰Mo(p,2n) on Small Medical Cyclotrons. *Phys. Procedia* **2015**, *66*, 383–395. [[CrossRef](#)]
14. Zyuzin, A.; Guérin, B.; van Lier, E.; Tremblay, S.; Rodrigue, S.; Rousseau, J.A.; Dumulon-Perreault, V.; Lecomte, R.; van Lier, J.E. Cyclotron Production of ^{99m}Tc. In Proceedings of the WTTC13, Roskilde, Denmark, 26–28 July 2010.
15. Avetisyan, A.; Dallakyan, R.; Sargsyan, R.; Melkonyan, A.; Mkrtchyan, M.; Harutyunyan, G.; Dobrovolsky, N. The powdered molybdenum target preparation technology for ^{99m}Tc production on C18 cyclotron. *IJEIT* **2015**, *4*, 8.
16. Taghilo, M. Cyclotron production of ⁸⁹Zr: A potent radionuclide for positron emission tomography. *Int. J. Phys. Sci.* **2012**, *7*. [[CrossRef](#)]
17. Morley, T.J.; Penner, L.; Schaffer, P.; Ruth, T.J.; Bénard, F.; Asselin, E. The deposition of smooth metallic molybdenum from aqueous electrolytes containing molybdate ions. *Electrochem. Commun.* **2012**, *15*, 78–80. [[CrossRef](#)]
18. Kazimierzak, H.; Ozga, P.; Socha, R.P. Investigation of electrochemical co-deposition of zinc and molybdenum from citrate solutions. *Electrochimica Acta* **2013**, *104*, 378–390. [[CrossRef](#)]
19. Queern, S.L.; Aweda, T.A.; Massicano, A.V.F.; Clanton, N.A.; El Sayed, R.; Sader, J.A.; Zyuzin, A.; Lapi, S.E. Production of Zr-89 using sputtered yttrium coin targets. *Nucl. Med. Biol.* **2017**, *50*, 11–16. [[CrossRef](#)] [[PubMed](#)]
20. Meijs, W.E.; Herscheid, J.D.M.; Haisma, H.J.; Wijbrandts, R.; van Langevelde, F.; Van Leuffen, P.J.; Mooy, R.; Pinedo, H.M. Production of highly pure no-carrier added ⁸⁹Zr for the labelling of antibodies with a positron emitter. *Appl. Radiat. Isot.* **1994**, *45*, 1143–1147. [[CrossRef](#)]
21. Verel, I.; Visser, G.W.M.; Boellaard, R.; Walsum, M.S.; Snow, G.B.; Dongen, G.A.M.S. van ⁸⁹Zr Immuno-PET: Comprehensive Procedures for the Production of ⁸⁹Zr-Labeled Monoclonal Antibodies. *J. Nucl. Med.* **2003**, *44*, 1271–1281.
22. Jalilian, A.; Targholizadeh, H.; Raisali, G.; Zandi, H.; Kamali Dehgan, M. Direct Technetium radiopharmaceuticals production using a 30MeV Cyclotron. *DARU J. Fac. Pharm. Tehran Univ. Med. Sci.* **2011**, *19*, 187–192.

23. Maier, H.J.; Friebel, H.U.; Frischke, D.; Grossmann, R. State of the art of high vacuum sputter deposition of nuclear accelerator targets. *Nucl. Instrum. Methods Phys. Res. Sect. Accel. Spectrometers Detect. Assoc. Equip.* **1993**, *334*, 137–141. [[CrossRef](#)]
24. Folger, H.; Klemm, J.; Muller, M. Preparation of Nuclear Accelerator Targets by Focused Ion Beam Sputter Deposition. *IEEE Trans. Nucl. Sci.* **1983**, *30*, 1568–1572. [[CrossRef](#)]
25. Esposito, J.; Bettoni, D.; Boschi, A.; Calderolla, M.; Cisternino, S.; Fiorentini, G.; Keppel, G.; Martini, P.; Maggiore, M.; Mou, L.; et al. LARAMED: A Laboratory for Radioisotopes of Medical Interest. *Molecules* **2019**, *24*, 20. [[CrossRef](#)]
26. Esposito, J.; Vecchi, G.; Pupillo, G.; Taibi, A.; Uccelli, L.; Boschi, A.; Gambaccini, M. Evaluation of Mo 99 and Tc 99 m Productions Based on a High-Performance Cyclotron. *Sci. Technol. Nucl. Install.* **2013**, *2013*, 1–14. [[CrossRef](#)]
27. Boschi, A.; Martini, P.; Pasquali, M.; Uccelli, L. Recent achievements in Tc-99m radiopharmaceutical direct production by medical cyclotrons. *Drug Dev. Ind. Pharm.* **2017**, *43*, 1402–1412. [[CrossRef](#)]
28. Martini, P.; Boschi, A.; Cicoria, G.; Zagni, F.; Corazza, A.; Uccelli, L.; Pasquali, M.; Pupillo, G.; Marengo, M.; Loriggiola, M.; et al. In-house cyclotron production of high-purity Tc-99m and Tc-99m radiopharmaceuticals. *Appl. Radiat. Isot.* **2018**, *139*, 325–331. [[CrossRef](#)]
29. Uzunov, N.M.; Melendez-Alafort, L.; Bello, M.; Cicoria, G.; Zagni, F.; De Nardo, L.; Selva, A.; Mou, L.; Rossi-Alvarez, C.; Pupillo, G.; et al. Radioisotopic purity and imaging properties of cyclotron-produced ^{99m}Tc using direct ¹⁰⁰Mo(p, 2 n) reaction. *Phys. Med. Biol.* **2018**, *63*, 185021. [[CrossRef](#)]
30. Martini, P.; Boschi, A.; Cicoria, G.; Uccelli, L.; Pasquali, M.; Duatti, A.; Pupillo, G.; Marengo, M.; Loriggiola, M.; Esposito, J. A solvent-extraction module for cyclotron production of high-purity technetium-99m. *Appl. Radiat. Isot.* **2016**, *118*, 302–307. [[CrossRef](#)]
31. van de Watering, F.C.J.; Rijpkema, M.; Perk, L.; Brinkmann, U.; Oyen, W.J.G.; Boerman, O.C. Zirconium-89 Labeled Antibodies: A New Tool for Molecular Imaging in Cancer Patients. *BioMed Res. Int.* **2014**, *2014*, 1–13. [[CrossRef](#)]
32. Jalilian, A.R.; Osso, J.A. Production, applications and status of zirconium-89 immunoPET agents. *J. Radioanal. Nucl. Chem.* **2017**, *314*, 7–21. [[CrossRef](#)]
33. Kasbollah, A.; Eu, P.; Cowell, S.; Deb, P. Review on Production of ⁸⁹Zr in a Medical Cyclotron for PET Radiopharmaceuticals. *J. Nucl. Med. Technol.* **2013**, *41*, 35–41. [[CrossRef](#)]
34. Severin, G.W.; Engle, J.W.; Nickles, R.J.; Barnhart, T.E. ⁸⁹Zr Radiochemistry for PET. *Med. Chem. Shariqah United Arab Emir.* **2011**, *7*, 389–394.
35. Thornton, J.A. Influence of apparatus geometry and deposition conditions on the structure and topography of thick sputtered coatings. *J. Vac. Sci. Technol.* **1974**, *11*, 666–670. [[CrossRef](#)]
36. Hoffman, D.W.; Thornton, J.A. Internal stresses in sputtered chromium. *Thin Solid Films* **1977**, *40*, 355–363. [[CrossRef](#)]
37. Cicoria, G.; Pancaldi, D.; Piancastelli, L.; Giovaniello, G.; Bianconi, D.; Bollini, D.; Menapace, E.; Givollani, S.; Pettinato, C.; Spinelli, A.; et al. Marengo Development and Operational Test of a Solid Target for the Pettrace Cyclotron. In Proceedings of the 13th European Symposium on Radiopharmacy and Radiopharmaceuticals, Lucca, Italy, 30 March–2 April 2006; pp. 3–4.
38. Ciarmatori, A.; Cicoria, G.; Pancaldi, D.; Infantino, A.; Boschi, S.; Fanti, S.; Marengo, M. Some experimental studies on ⁸⁹Zr production. *Radiochim. Acta* **2011**, *99*, 631–634. [[CrossRef](#)]
39. Radionuclide Yield Calculator - ARRONAX. Available online: <http://www.cyclotron-nantes.fr/spip.php?article373> (accessed on 12 March 2019).
40. James Ziegler - SRIM & TRIM. Available online: <http://www.srim.org/> (accessed on 12 March 2019).
41. EXFOR: Experimental Nuclear Reaction Data. Available online: <https://www.nndc.bnl.gov/exfor/exfor.htm> (accessed on 12 March 2019).
42. Omara, H.M.; Hassan, K.F.; Kandil, S.A.; Hegazy, F.E.; Saleh, Z.A. Proton induced reactions on ⁸⁹Y with particular reference to the production of the medically interesting radionuclide ⁸⁹Zr. *Radiochim. Acta* **2009**, *97*. [[CrossRef](#)]
43. Sathesh, B.; Musthafa, M.M.; Singh, B.P.; Prasad, R. NUCLEAR ISOMERS ^{90m, g}Zr, ^{89m, g}Zr, ^{89m, g}Y AND ^{85m, g}Sr FORMED BY BOMBARDMENT OF ⁸⁹Y WITH PROTONS OF ENERGIES FROM 4 TO 40 MeV. *Int. J. Mod. Phys. E* **2011**, *20*, 2119–2131. [[CrossRef](#)]

44. Wenrong, Z.; Qingbiao, S.; Hanlin, L.; Weixiang, Y. Investigation of $^{89}\text{Y}(p,n)^{89}\text{Zr}$, $^{89}\text{Y}(p,2n)^{88}\text{Zr}$ and $^{89}\text{Y}(p,pn)^{88}\text{Y}$ reactions up to 22 MeV. *Chin. J. Nucl. Phys.* **1992**, *14*, 7–14.
45. Otuka, N.; Takács, S. Definitions of radioisotope thick target yields. *Radiochim. Acta* **2015**, *103*, 1–6. [[CrossRef](#)]
46. Detor, A.J.; Hodge, A.M.; Chason, E.; Wang, Y.; Xu, H.; Conyers, M.; Nikroo, A.; Hamza, A. Stress and microstructure evolution in thick sputtered films. *Acta Mater.* **2009**, *57*, 2055–2065. [[CrossRef](#)]
47. Vink, T.J.; Somers, M.A.J.; Daams, J.L.C.; Dirks, A.G. Stress, strain, and microstructure of sputter-deposited Mo thin films. *J. Appl. Phys.* **1991**, *70*, 4301–4308. [[CrossRef](#)]
48. Karabacak, T.; Senkevich, J.J.; Wang, G.-C.; Lu, T.-M. Stress Reduction in Sputter Deposited Thin Films Using Physically Self-Assembled Nanostructures as Compliant Layers. *Th Annu. Tech. Conf. Proc.* **2004**, *16*.
49. Palmieri, V.; Skliarova, H.; Cisternino, S.; Marengo, M.; Cicoria, G. Method for Obtaining a Solid Target for Radiopharmaceuticals Production. International Patent Application PCT/IB2018/056826, 7 September 2018. National Institute of Nuclear Physics, deposition reference P1183PC00.
50. Dabkowski, A.M.; Paisey, S.J.; Talboys, M.; Marshall, C. Optimization of Cyclotron Production for Radiometal of Zirconium 89. *Acta Phys. Pol. A* **2015**, *127*, 1479–1482. [[CrossRef](#)]
51. Wooten, A.; Madrid, E.; Schweitzer, G.; Lawrence, L.; Mebrahtu, E.; Lewis, B.; Lapi, S. Routine Production of ^{89}Zr Using an Automated Module. *Appl. Sci.* **2013**, *3*, 593–613. [[CrossRef](#)]
52. Lin, M.; Mukhopadhyay, U.; Waligorski, G.J.; Balatoni, J.A.; González-Lepera, C. Semi-automated production of ^{89}Zr -oxalate/ ^{89}Zr -chloride and the potential of ^{89}Zr -chloride in radiopharmaceutical compounding. *Appl. Radiat. Isot.* **2016**, *107*, 317–322. [[CrossRef](#)]
53. Poniger, S.; Tochon-Danguy, H.; Panopoulos, H.; Scott, A. Fully Automated Production of ^{89}Zr using IBA Nirta and Pinctada Systems. Available online: <http://hzdr.qucosa.de/api/qucosa%3A22272/attachment/ATT-0/> (accessed on 12 March 2019).



© 2019 by the authors. Licensee MDPI, Basel, Switzerland. This article is an open access article distributed under the terms and conditions of the Creative Commons Attribution (CC BY) license (<http://creativecommons.org/licenses/by/4.0/>).